

Half-Chain Entanglement Entropy in the One-Dimensional Spinless Fermion Model

Myung-Hoon Chung^a

College of Science and Technology, Hongik University, Sejong 339-701, Korea

(Dated: October 18, 2016)

Abstract

We calculate the half-chain entanglement entropy of the ground state in the one-dimensional spinless fermion model. Considering a tiny corner of the Hilbert space represented by matrix product states, we efficiently find the ground state by the infinite time-evolving block decimation. The Schmidt coefficients are used to determine the half-chain entanglement entropy. Using the bond dimension scaling of the half-chain entanglement entropy, we find the critical region, which is consistent with the previous results.

PACS numbers: 71.27.+a, 02.70.-c, 03.67.-a

^a To whom correspondence should be addressed.

E-mail address: mhchung@hongik.ac.kr

I. INTRODUCTION

In addition of quantum Monte Carlo [1] and exact diagonalization [2], the method of tensor networks [3] is one of the powerful theoretical tools to study strongly correlated many-body systems. Tensor network algorithms are based on the density-matrix renormalization group (DMRG) [4]. DMRG has proven to be a great success in the simulation of strongly correlated one-dimensional quantum lattice systems. The method of tensor network states has become popular after we found that the internal structure of DMRG can be understood with respect to the matrix product states (MPS) [5, 6]. For two-dimensional systems, the projected entangled-pair states (PEPS) [7] are introduced. More generally, there are many tensor network states (TNS), which include MPS, PEPS, tree tensor network states [8], the multiscale entanglement renormalization ansatz (MERA) [9], matrix-product projected states [10], and projected entangled simplex states (PESS) [11]. These tensor network states are used as the basis set for variational approaches to quantum many-body systems.

When a total Hamiltonian is written as a sum of local Hamiltonians, Vidal introduced a powerful method called time-evolving block decimation (TEBD) [12, 13] to find the ground state. If the total Hamiltonian has a symmetry such as translational invariance, we can use the so-called infinite TEBD (iTEBD) [14], in which we assume that the tensors in the TNS have the same form, and we update a few tensors to achieve the ground state.

Entanglement is a truly quantum mechanical phenomenon [15]. One of the recent interests in theoretical condensed matter physics is to understand entanglement [16] in strongly correlated quantum many-body systems. In fact, the entanglement entropy is used to characterize quantum phases [17, 18]. To define the entanglement entropy, we divide the quantum system into two parts A and B . We introduce a density matrix $\rho = |\Psi\rangle\langle\Psi|$ with a pure quantum state $|\Psi\rangle$ for the whole system, and obtain the reduced density matrix of subsystem A such as $\rho_A = \text{Tr}_B \rho$ by tracing out subsystem B . The entanglement entropy is the von Neumann entropy, which is given by $S_A = -\text{Tr}(\rho_A \log_2 \rho_A)$. In particular, for $1 + 1$ -dimensional quantum systems, the half-chain entanglement entropy [19] is defined by using the Schmidt coefficients. The entanglement entropy for a finite block of a $1 + 1$ -dimensional critical system was calculated analytically by using conformal field theory [20].

The purpose of this paper is to find the half-chain entanglement entropy in the one-dimensional spinless fermion model. To do so, we start by using the ansatz of matrix

product state for the ground state in the model. We present a slightly modified method in determining the ground state energy by normalizing the maximum Schmidt coefficient [21]. We apply our method to the one-dimensional spinless fermion model. We also find the finite bond dimension scaling of the half-chain entanglement entropy. The scaling behavior is consistent with the formula of the entanglement entropy given by Calabrese and Cardy [20].

This paper is organized as follows. In Sec. 2, a brief description of our method is given, and we present the role of the maximum Schmidt coefficient in determining the ground state energy. In Sec. 3, by using iTEBD, we calculate the ground state for the one-dimensional spinless fermion model. In Sec. 4, we present the numerical results, which are the half-chain entanglement entropy, and the corresponding data collapse. We find that the entanglement entropy shows abrupt changes on the boundary of phases. In conclusion, we discuss the future goal of simulating the two-dimensional fermion model, where we encounter notorious difficulties in relation with the negative sign problem.

II. METHOD

We briefly review the method [21] that we use here for completeness. There are two methods to obtain the ground state in tensor network algorithms. One is the variational method, in which we minimize the energy expectation value by changing parameters in the ansatz. The other is the imaginary time evolving, which produces the ground state energy by applying an operator on a tensor network state consecutively. The imaginary time evolving method is adopted here to find the ground state.

The imaginary time evolving method starts by considering the formal solution $|\Psi(T)\rangle$ to the imaginary time Schrödinger equation, which is written as

$$|\Psi(T)\rangle = \exp\{-(H - E)T\}|\Psi(0)\rangle = \prod_{\tau=0}^{T/\tau} \exp\{E\tau\} \exp(-H\tau)|\Psi(0)\rangle, \quad (1)$$

where we introduce an energy shift E for a given Hamiltonian H , and we will perform the Suzuki-Trotter decomposition for $\exp(-H\tau)$, where the Trotter time step τ should be sufficiently small. As the imaginary time T goes to infinity, the state $|\Psi(T)\rangle$ becomes the ground state for properly chosen E . In fact, when E is larger or smaller than the ground-state energy, $|\Psi(T)\rangle$ blows up or shrinks down, respectively, in the limit as $T \rightarrow \infty$. In a

numerical approach, we redefine E as a function of T to maintain the norm of state.

For one-dimensional systems, our ansatz for the ground state is a MPS because of the area law [16]. A tensor in MPS, A_{ab}^σ , has three indices, among which the physical index σ takes a value from 0 to $d - 1$. For the internal bond degree of freedom, the indices a (left) and b (right) run from 0 to $\chi - 1$, where χ is the bond dimension. The Schmidt coefficients between A_{ab}^σ and B_{bc}^ρ are denoted by λ_b^{AB} . A state in the space of the matrix product states is written as

$$|\text{MPS}\rangle = \sum_{\dots\sigma\rho\nu\eta\dots} \text{Tr}(\dots\lambda_a^{XA} A_{ab}^\sigma \lambda_b^{AB} B_{bc}^\rho \lambda_c^{BC} C_{cd}^\nu \lambda_d^{CD} D_{de}^\eta \dots) |\dots\sigma\rho\nu\eta\dots\rangle, \quad (2)$$

where Tr means that all internal bond indices a, b, c, d, \dots are summed up.

Vidal proposed a clever idea of TEBD for updating the tensors in the MPS of Eq. (2). Usually a local Hamiltonian is written as a sum of the elementary operators h_{ij} such as $H = \sum_{ij} h_{ij}$, where the index of i and j represents nearby sites. Then, by the Suzuki-Trotter decomposition, it is enough to consider the effect of $\exp(-h_{ij}\tau)$. When $\exp(-h_{ij}\tau)$ acts on the previous MPS, we approximate the output state into our new MPS by updating the tensors and the Schmidt coefficients locally. In fact, the first step in TEBD is to find the four-index tensor M defined by

$$M_{\sigma_i\sigma_j}^{\rho_i\rho_j} = \langle\rho_i\rho_j|\exp(-h_{ij}\tau)|\sigma_i\sigma_j\rangle. \quad (3)$$

For example, in order to update A , B , and λ^{AB} in $|\text{MPS}\rangle$ of Eq. (2), we consider the four-index tensor Θ :

$$\Theta_{ac}^{\rho_i\rho_j} = \sum_{b=0}^{\chi-1} \sum_{\sigma_i,\sigma_j=0}^{d-1} \lambda_a^{XA} A_{ab}^{\sigma_i} \lambda_b^{AB} B_{bc}^{\sigma_j} \lambda_c^{BC} M_{\sigma_i\sigma_j}^{\rho_i\rho_j}. \quad (4)$$

By employing singular value decompositions (SVD), we obtain the updated $\tilde{\lambda}_b^{AB}$ by keeping the χ largest weights:

$$\Theta_{ac}^{\rho_i\rho_j} \rightarrow \sum_{b=0}^{\chi-1} \bar{A}_{ab}^{\rho_i} \tilde{\lambda}_b^{AB} \bar{B}_{bc}^{\rho_j} = \sum_{b=0}^{\chi-1} \lambda_a^{XA} \tilde{A}_{ab}^{\rho_i} \tilde{\lambda}_b^{AB} \tilde{B}_{bc}^{\rho_j} \lambda_c^{BC}. \quad (5)$$

By dividing and attaching the weights, we find \tilde{A} and \tilde{B} from \bar{A} and \bar{B} in the above. We denote this process graphically as follows:

$$\begin{array}{c} - \quad \Theta \quad - \quad \rightarrow \quad - \quad \tilde{A} \quad - \quad \tilde{B} \quad - \\ | \quad | \quad \quad \quad | \quad | \end{array}$$

where the vertical lines mean the physical indices. A similar procedure is performed for other tensors C , D , \dots and other weights on the bonds. We note that it is possible to update the tensors simultaneously if we use multi-core computers. If there is a translational symmetry in the local Hamiltonian, we use iTEBD, where we assume that only two matrices A and B repeat in the MPS. In this case, we need to update A , B , λ^{AB} , and λ^{BA} only.

Now we present how to determine the ground state energy without evaluations of inner products [22]. Being inspired by the diffusion Monte Carlo [1, 23], we have introduced the energy E in front of the operator of the Suzuki-Trotter decomposition in Eq. (1). While the energy is adjusted by controlling the number of replicas in the diffusion Monte Carlo, here we determine E by managing the factor in front of the wave function [22]. The algorithm is as follows: when a typical operator $\exp(-h_{ij}\tau)$ acts on a matrix product state $|\text{MPS}\rangle$, we perform SVD and obtain χ singular values of $\lambda_0 \geq \lambda_1 \geq \dots \geq \lambda_{\chi-1}$. We take out the maximum λ_0 and place it in front of the wave function, and we modify the singular values as follows: $1 \geq \lambda_1/\lambda_0 \geq \dots \geq \lambda_{\chi-1}/\lambda_0$. In this way, we normalize $|\text{MPS}\rangle$ such that all weights on each bond have the maximum value of 1. Thus, whenever the weights are modified by $\exp(-H\tau)$ acting on the k -th time step state $|\text{MPS}_k\rangle$, we take out the maximum weight to obtain the factor F in front of the state

$$\exp(-H\tau)|\text{MPS}_k\rangle = F|\text{MPS}_{k+1}\rangle, \quad (6)$$

where the maximum Schmidt coefficient on each bond in $|\text{MPS}_{k+1}\rangle$ is equal to 1. We obtain the factor F by multiplying the previous F by λ_0 whenever any bond is modified. Because we require no divergence and no convergence to zero for the state, as in the diffusion Monte Carlo, we adjust the next energy value E_{k+1} for the state to be stable in this way:

$$E_{k+1} = -\frac{\log F}{\tau}. \quad (7)$$

After we find E_{k+1} , we set $F = 1$ again for the next iteration in the computer simulation. We note that during the time evolution, E_k is stable and approaches the ground-state energy in the limit of $k \rightarrow \infty$. The solution of $|\text{MPS}_\infty\rangle$ is also stable.

III. ONE-DIMENSIONAL SPINLESS FERMION MODEL

In relation with the Luttinger liquids, the spinless fermion model may be the simplest fermion system, which is a good laboratory for a benchmark calculation [22]. We begin by

presenting the Hamiltonian for the one-dimensional spinless fermion model:

$$H = -t \sum_i (c_i^\dagger c_{i+1} + c_{i+1}^\dagger c_i) + V \sum_i (n_i - \frac{1}{2})(n_{i+1} - \frac{1}{2}) - \mu \sum_i n_i, \quad (8)$$

where t is the nearest-neighbor hopping strength in a one-dimensional lattice, V is the nearby Coulomb interaction strength, and n_i is the number operator. The role of the chemical potential μ is to control the number of fermions in the system. Because this one-dimensional spinless fermion model preserves the translational invariance, we can use iTEBD here.

When we apply iTEBD to find the ground state, we divide the Hamiltonian into two parts, which are denoted by e (even) and o (odd), such as $H = H_e + H_o = \sum_j h_{2j} h_{2j+1} + \sum_j h_{2j+1} h_{2j+2}$ for the Suzuki-Trotter decomposition. The elementary operators $h_{i \ i+1}$ are written as

$$h_{i \ i+1} = -t(c_i^\dagger c_{i+1} + c_{i+1}^\dagger c_i) + V(n_i - \frac{1}{2})(n_{i+1} - \frac{1}{2}) - \frac{\mu}{2}n_i - \frac{\mu}{2}n_{i+1}. \quad (9)$$

In order to find the ground state, we consider a tiny corner of the Hilbert space. The tiny corner is characterized by the MPS with two tensors and two vectors with a fixed bond dimension χ .

It is natural to define the physical index σ_i in the MPS for the spinless fermion model. The state on the i -th site is represented by $\sigma_i = 0$ or 1 , such as 0 for the vacancy and 1 for the occupancy. The state of the Fock space is written in terms of the creation operators c_i^\dagger as follows:

$$|\sigma_0 \cdots \sigma_{L-1}\rangle = (c_0^\dagger)^{\sigma_0} \cdots (c_{L-1}^\dagger)^{\sigma_{L-1}} |0\rangle. \quad (10)$$

Now we apply iTEBD in order to obtain the ground state of the Hamiltonian of Eq. (8). In the process of iTEBD, we need to determine $\langle \rho_i \rho_{i+1} | \exp(-h_{i \ i+1} \tau) | \sigma_i \sigma_{i+1} \rangle$. We first calculate the 4×4 matrix $\langle \rho_i \rho_{i+1} | (-h_{i \ i+1}) | \sigma_i \sigma_{i+1} \rangle$, which is written as

$$\begin{pmatrix} -\frac{1}{4}V & 0 & 0 & 0 \\ 0 & \frac{1}{4}V + \frac{1}{2}\mu & t & 0 \\ 0 & t & \frac{1}{4}V + \frac{1}{2}\mu & 0 \\ 0 & 0 & 0 & -\frac{1}{4}V + \mu \end{pmatrix}$$

By using the Taylor expansion, the four-index tensor M of $\langle \rho_i \rho_{i+1} | \exp(-h_{i \ i+1} \tau) | \sigma_i \sigma_{i+1} \rangle$ is written in terms of $\langle \rho_i \rho_{i+1} | (-h_{i \ i+1} \tau) | \sigma_i \sigma_{i+1} \rangle$. We obtain the values of M numerically for given t , V , μ , and τ . For a small τ , it is enough to make the Taylor expansion up to $\mathcal{O}(\tau^7)$.

Performing iTEBD with the MPS, we use two matrices A , B and two Schmidt coefficients λ^{AB} , λ^{BA} . Our goal is to find $|\text{MPS}\rangle$ for the ground state by optimizing A and B in iTEBD. We describe the procedure for the computational simulation of iTEBD from the Suzuki-Trotter decomposition with $H = H_e + H_o$:

1. Choose A , B , λ^{AB} , and λ^{BA} randomly.
2. Update A , λ^{AB} , and B , by handling H_e .
3. Update B , λ^{BA} , and A , by handling H_o .
4. Repeat from step 2 until λ^{AB} and λ^{BA} are identical.

From Eq. (7), we note that the corresponding energy per site e is given by

$$e = -\frac{\log(\lambda_0^{AB}\lambda_0^{BA})}{2\tau}, \quad (11)$$

where λ_0^{AB} and λ_0^{BA} are the maximum singular values obtained by performing SVD. As a benchmark calculation, we present the ground state energy per site for the model as shown in Fig 1.

IV. NUMERICAL RESULTS: HALF-CHAIN ENTANGLEMENT ENTROPY

When we find the ground state as a form of MPS, the advantage of MPS is easily to extract the half-chain entanglement entropy [19]. We present the von Neumann entropy for the half-infinite chain by using the Schmidt coefficients:

$$S_h = -\sum_{i=0}^{\chi-1} \lambda_i^2 \log \lambda_i^2, \quad \lambda_i = \frac{\lambda_i^{AB}}{\sqrt{\sum_i |\lambda_i^{AB}|^2}}. \quad (12)$$

We note that we do not have to distinguish λ_i^{BA} from λ_i^{AB} in $|\text{MPS}_\infty\rangle$ because we simulate until they become equal. By simulation with randomly chosen initial states for the model, we repeatedly find two ground states whose energy difference is invisible, in fact, less than 10^{-5} . Thus, it is hard to distinguish two states by energy. However, two states prominently have different entanglement entropies. We show two kinds of the corresponding half-chain entanglement entropy S_h in Fig. 2 for the bond dimension $\chi = 28$. The shapes of entropy are similar, but the values are quite different from each other.

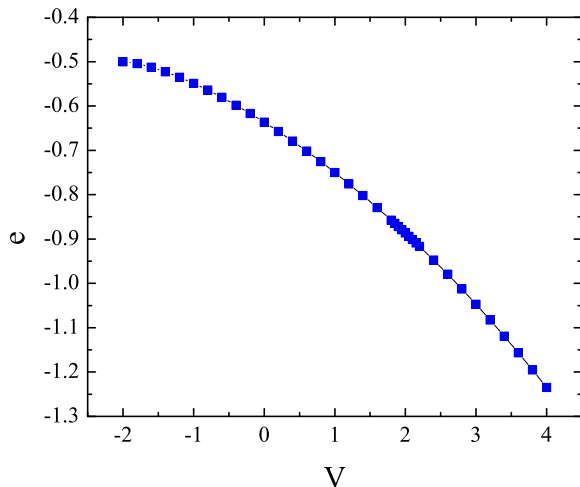


FIG. 1. The ground state energy per site e versus V . We observe that the energy values are almost identical for sufficiently large χ . We find the smooth behavior near $V = 2$. We fix the parameters as $t = 1$, $\mu = 0$, and $\tau = 0.02$.

Focusing on the less entangled state which is lower in Fig. 2, we present the half-chain entanglement entropy for several internal bond dimensions χ in Fig. 3. We find the abrupt changes [22] near $V = 2$ and $V = -2$. For $V > 2$, the entanglement entropy becomes saturated, in other words, the entropy does not depend on χ . This suggests that the corresponding Hamiltonian is gapped. On the other hand, for $-2 < V < 2$, as χ increases, the entropy also increases. This χ -dependence is the signal of criticality or gapless.

It is remarkable that the entanglement entropy for a critical system can be obtained by means of conformal field theory. For the case where the whole one-dimensional system has a finite but large length L with the periodic boundary condition and the subsystem is a single interval of length l , the entanglement entropy [20] is given by

$$S_l = \frac{c}{3} \log\left(\frac{L}{\pi a} \sin\left(\frac{\pi l}{L}\right)\right) + c_1, \quad (13)$$

where a is the lattice spacing, c_1 is a non-universal constant, and c is the central charge.

Because there is only one side contact for the half-chain, we should modify the above

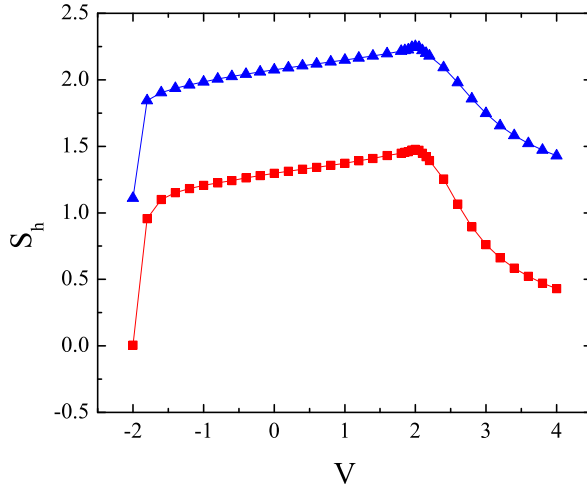


FIG. 2. The two kinds of the half-chain entanglement entropy S_h versus V for $\chi = 28$. We fix the parameters as $t = 1$, $\mu = 0$, and $\tau = 0.02$. We note that simulation is unstable near $V = -2$ because of strong attraction between fermions.

formula for the half-chain entanglement entropy by dividing 2 and setting $l = L/2$ such as

$$S_h = \frac{c}{6} \log(L) + c'_1, \quad (14)$$

where c'_1 is a non-universal constant. The length of the system size L is related to the correlation length ξ near a critical point such as $L \sim \xi$. Furthermore, it is postulated that the correlation length ξ has the scaling relation with the bond dimension χ such as $\xi \sim \chi^\kappa$ [19, 24]. Then, we find

$$S_h(\chi) = \frac{c\kappa}{6} \log(\chi) + c''_1. \quad (15)$$

Using this formula, it is of interest to check the finite χ scaling of S_h . We find the data collapse in the plot of $6(S_h - c''_1)/\log(\chi)$ versus V by adjusting c''_1 as shown in Fig 4. The data collapse happens between $V = -2$ and $V = 2$, which is consistent with the previous results about the critical region. Finally, we determine the scaling exponent κ from the data collapse of Fig 4, for instance, $\kappa = 1.47(1)$ at $V = 2$ with the well-known result of $c = 1$ [25].

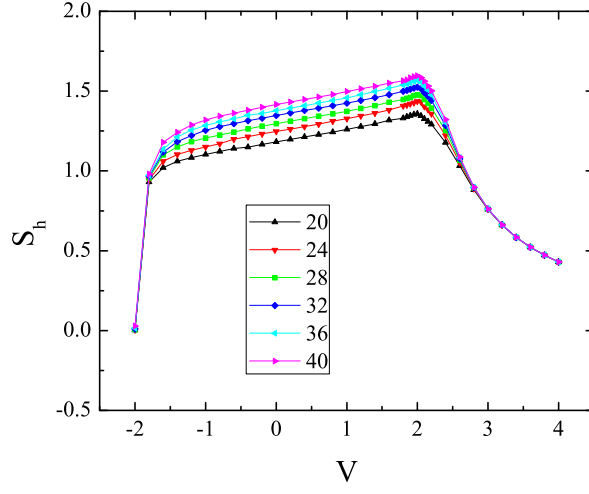


FIG. 3. The half-chain entanglement entropy S_h versus V for several χ from 20 to 40. We fix the parameters as $t = 1$, $\mu = 0$, and $\tau = 0.02$.

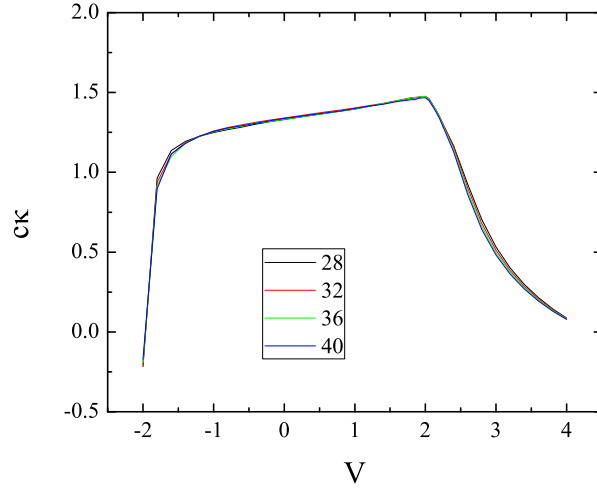


FIG. 4. The plot of $6(S_h - c_1'')/\log(\chi)$ versus V with $\chi = 28, 32, 36, 40$ for the system of $t = 1$, $\mu = 0$, and $\tau = 0.02$. We fix the non-universal c_1'' as $c_1'' = 0.23 + 0.025V$.

V. CONCLUSION

In summary, we have presented the half-chain entanglement entropy for the spinless fermion model. We perform the finite bond dimension scaling with the entanglement entropy. We find the critical behavior between $V = -2$ and $V = 2$, which is consistent with the previous results.

When we use multi-core computers, it is possible to parallelize the local updates of the internal bonds for the model of no translational symmetry. As a future work, we hope that someone will perform this parallel computing soon.

It is of interest to extend our method to two-dimensional systems. Although we do not encounter the notorious sign problem here, we have to overcome the sign problem in the two-dimensional model with PEPS. We anticipate progress in the two-dimensional case.

ACKNOWLEDGMENTS

This work was partially supported by the Basic Science Research Program through the National Research Foundation of Korea (NRF) funded by the Ministry of Education, Science and Technology (Grant No. 2011-0023395). The author would like to thank M.C. Cha and J.W. Lee for helpful discussions.

-
- [1] D. Ceperley and B. Alder, *Science* **231**, 555 (1986).
 - [2] E. Dagotto, *Rev. Mod. Phys.* **66**, 763 (1994).
 - [3] R. Orus, *Ann. Phys.* **349**, 117 (2014).
 - [4] S. White, *Phys. Rev. Lett.* **69**, 2863 (1992).
 - [5] S. Östlund and S. Rommer, *Phys. Rev. Lett.* **75**, 3537 (1995).
 - [6] U. Schollwöck, *Ann. Phys.* **326**, 96 (2011).
 - [7] D. Pérez-García, F. Verstraete, M. M. Wolf, and J. I. Cirac, *Quant. Inf. Comp.* **8**, 0650 (2008).
 - [8] V. Murg, F. Verstraete, Ó. Legeza, and R. M. Noack, *Phys. Rev. B* **82**, 205105 (2010).
 - [9] G. Vidal, *Phys. Rev. Lett.* **99**, 220405 (2007).
 - [10] C. P. Chou, F. Pollmann, and T. K. Lee, *Phys. Rev. B* **86**, 041105 (2012).

- [11] Z. Xie, J. Chen, J. F. Yu, X. Kong, B. Normand, and T. Xiang, *Phys. Rev. X* **4**, 011025 (2014).
- [12] G. Vidal, *Phys. Rev. Lett.* **91**, 147902 (2003).
- [13] G. Vidal, *Phys. Rev. Lett.* **93**, 040502 (2004).
- [14] G. Vidal, *Phys. Rev. Lett.* **98**, 070201 (2007).
- [15] R. Horodecki, P. Horodecki, M. Horodecki, and K. Horodecki, *Rev. Mod. Phys.* **81**, 865 (2009).
- [16] J. Eisert, M. Cramer, and M. B. Plenio, *Rev. Mod. Phys.* **82**, 277 (2010).
- [17] Y. Chen, P. Zanardi, Z. D. Wang, and F. C. Zhang, *New J. Phys.* **8**, 97 (2006).
- [18] M. H. Chung and D. P. Landau, *Phys. Rev. B* **83**, 113104 (2011).
- [19] L. Tagliacozzo, T. R. de Oliveira, S. Iblisdir, and J. I. Latorre, *Phys. Rev. B* **78**, 024410 (2008).
- [20] P. Calabrese and J. Cardy, *J. Stat. Mech.*, P06002 (2004).
- [21] S. Park and M. Cha, *J. Korean Phys. Soc.* **67**, 1619 (2015).
- [22] M. H. Chung, *J. Korean Phys. Soc.* **64**, 999 (2014).
- [23] M. H. Chung and D. P. Landau, *Phys. Rev. B* **85**, 115115 (2012).
- [24] F. Pollmann, S. Mukerjee, A. M. Turner, J. E. Moore, *Phys. Rev. Lett.* **102**, 255701 (2009).
- [25] S. Nishimoto, *Phys. Rev. B* **84**, 195108 (2011).